

Review

# Graphene Nanocomposites for Electromagnetic Interference Shielding—Trends and Advancements

Ayesha Kausar <sup>1,2,\*</sup> , Ishaq Ahmad <sup>1,2</sup>, Tingkai Zhao <sup>1,3</sup>, Osamah Aldaghri <sup>4</sup> , Khalid H. Ibnaouf <sup>4</sup> , M. H. Eisa <sup>4</sup> and Tran Dai Lam <sup>5</sup> 

- <sup>1</sup> NPU-NCP Joint International Research Center on Advanced Nanomaterials and Defects Engineering, Northwestern Polytechnical University, Xi'an 710072, China
- <sup>2</sup> UNESCO-UNISA Africa Chair in Nanosciences/Nanotechnology, iThemba LABS, Somerset West 7129, South Africa
- <sup>3</sup> School of Materials Science & Engineering, Northwestern Polytechnical University, Xi'an 710072, China
- <sup>4</sup> Department of Physics, College of Science, Imam Mohammad Ibn Saud Islamic University (IMSIU), Riyadh 13318, Saudi Arabia
- <sup>5</sup> Institute for Tropical Technology, Vietnam Academy of Science and Technology, 18 Hoang Quoc Viet, Cau Giay, Hanoi 100000, Vietnam
- \* Correspondence: dr.ayeshakausar@yahoo.com

**Abstract:** Electromagnetic interference is considered a serious threat to electrical devices, the environment, and human beings. In this regard, various shielding materials have been developed and investigated. Graphene is a two-dimensional, one-atom-thick nanocarbon nanomaterial. It possesses several remarkable structural and physical features, including transparency, electron conductivity, heat stability, mechanical properties, etc. Consequently, it has been used as an effective reinforcement to enhance electrical conductivity, dielectric properties, permittivity, and electromagnetic interference shielding characteristics. This is an overview of the utilization and efficacy of state-of-the-art graphene-derived nanocomposites for radiation shielding. The polymeric matrices discussed here include conducting polymers, thermoplastic polymers, as well as thermosets, for which the physical and electromagnetic interference shielding characteristics depend upon polymer/graphene interactions and interface formation. Improved graphene dispersion has been observed due to electrostatic, van der Waals,  $\pi$ - $\pi$  stacking, or covalent interactions in the matrix nanofiller. Accordingly, low percolation thresholds and excellent electrical conductivity have been achieved with nanocomposites, offering enhanced shielding performance. Graphene has been filled in matrices like polyaniline, polythiophene, poly(methyl methacrylate), polyethylene, epoxy, and other polymers for the formation of radiation shielding nanocomposites. This process has been shown to improve the electromagnetic radiation shielding effectiveness. The future of graphene-based nanocomposites in this field relies on the design and facile processing of novel nanocomposites, as well as overcoming the remaining challenges in this field.

**Keywords:** graphene; nanocomposite; dispersion; interaction; conductivity; EMI shielding



**Citation:** Kausar, A.; Ahmad, I.; Zhao, T.; Aldaghri, O.; Ibnaouf, K.H.; Eisa, M.H.; Lam, T.D. Graphene Nanocomposites for Electromagnetic Interference Shielding—Trends and Advancements. *J. Compos. Sci.* **2023**, *7*, 384. <https://doi.org/10.3390/jcs7090384>

Academic Editor: Francesco Tornabene

Received: 9 August 2023

Revised: 30 August 2023

Accepted: 6 September 2023

Published: 13 September 2023



**Copyright:** © 2023 by the authors. Licensee MDPI, Basel, Switzerland. This article is an open access article distributed under the terms and conditions of the Creative Commons Attribution (CC BY) license (<https://creativecommons.org/licenses/by/4.0/>).

## 1. Introduction

Graphene is a remarkable nanocarbon nanomaterial [1–3]. It possesses a unique structure and technically significant properties for polymeric matrices [4]. Adding very small amounts of graphene to polymers may cause significant improvements in their physical characteristics [5]. Graphene and derived nanomaterials have been applied in the fields of electromagnetic interference (EMI) shielding equipment, electronics and microelectronics, sensors and actuators, printing devices, energy devices, and other methodological and industrial applications [6]. Polymer/graphene nanocomposites have been found to be effective in overcoming the challenging aspects of electromagnetic wave interference [7]. In this regard, the amount, dispersion, and morphology of graphene and modified graphene

nanostructures in polymers are recognized as important variables. Moreover, superior interactions, compatibility, and interface formation between the polymer and graphene can enhance the effectiveness of the electromagnetic interference shielding (EMI SE) [8]. Functional graphene can effect excellent physical or covalent interfacial interactions [9,10]. The synergetic effect between polymers and graphene has been found to enhance the physical properties of such nanocomposites. Furthermore, interpenetrating networks have been developed in polymer/graphene nanomaterials, enabling superior electron mobilization and thereby improving the electromagnetic protection features.

This review stresses the essentials, design, and properties of EMI shielding polymer- and graphene-derived nanocomposites. The EMI shielding mechanism, mutual interactions, and interface formation are considered important factors in controlling the overall radiation protection performance of nanocomposites. Several conducting thermoplastics and thermosets have been applied in the fabrication of radiation defense materials with graphene. Accordingly, graphene, graphene oxide, and modified graphene have been used to improve EMI protection for polymers. This paper is a literature overview; it is intended to support the future development of innovative graphene-based materials for EMI shielding.

## 2. Graphene, Modified Forms, and Derived Nanocomposites

Graphene is an exceptional carbon nanoparticle material or nanocarbon nanomaterial. Single layer graphene has a one-atom-thick nanostructure made up of hexagonal carbon atoms [11–13]. The  $sp^2$  hybridized C-C linking gives rise to  $\pi$ -electron orbitals in graphene [14–16]. The material was discovered in 2004 [17]. After that, numerous top-down and bottom-up methods have been investigated for graphene synthesis [18–21]. Some commonly used graphene synthesis techniques include graphite mechanical cleavage, graphite exfoliation, organic synthesis, chemical vapor deposition, and several other methods [22–25]. Graphene has excellent transparency properties, allowing around 97–98% of the light it receives to pass through it [26,27]. Due to its delocalized nanostructure, graphene possesses an electron mobility of about  $200,000 \text{ cm}^2 \text{ V}^{-1} \text{ s}^{-1}$  [28]. Its thermal conductivity has been found to be in the range of 3000–5000 W/mK [29]. Moreover, graphene has a tensile strength and a Young's modulus of 130 GPa and 1 TPa, respectively [30]. Consequently, graphene is 200–300 times stronger than steel. Van der Waals forces usually occur between graphene layers [31–33]. The outstanding structural and physical properties of graphene give rise to technical applications in high performance nanocomposites and in the energy, electronics, civil, and aerospace fields [34]. Among the various functional forms of graphene, graphene oxide is considered especially important [35]. Graphene oxide has surface functional groups such as hydroxyl, epoxide, carbonyl, carboxyl acid, etc. Various approaches have been used for the functionalization of graphene [36]. Important techniques for non-covalent modification [37] and covalent functionalization [38] have been reported. In this paper, hydrothermal [39], solvothermal [40], electrochemical [41], electrophoresis [42], and physical deposition approaches [43] are discussed. Non-covalent functionalization usually incorporates inorganic or organic groups through aromatic stacking or electrostatic or hydrophobic linking on the graphene surface [44]. The covalent modification of graphene may involve the click chemistry mechanism [45], atom transfer radical polymerization [46], or an in situ chemical deposition of nanoparticles on the nanosheet surface [47]. Graphene oxide and reduced graphene oxide are especially important chemically modified forms of graphene [48]. For the formation of graphene oxide, a chemical or liquid phase exfoliation of graphite is commonly used. In the Brodie method, a mixture of potassium chlorate/nitric acid is used to form graphene oxide from graphite [49]. In the Hummers and Offeman method, potassium permanganate, sodium nitrate, and sulfuric acid are used to obtain graphene oxide from a graphite precursor [50]. Reduced graphene oxide is a further modified form of graphene oxide. In this context, chemical as well as thermal approaches have been used to convert graphene oxide to reduced graphene oxide [51]. Both graphene and its adapted forms have been studied in order to achieve

superior electrical conduction, thermal conduction, heat stability, and mechanical strength of nanomaterials [52–54].

Graphene has been amalgamated with polymers to form polymer/graphene nanocomposites, applied for electronics [55,56], sensors [57,58], energy devices [59], etc. Various straight forward and effective methods have been used to form polymer/graphene nanocomposites [60]. The solvent casting or mixing technique has been commonly applied to form the polymer/graphene nanocomposites [61]. It is a facile and cheap technique in which polymer is dissolved in solvent. Graphene is also dispersed in solvent and mixed with the polymer solution. Then, solution casting and evaporation lead to the formation of nanocomposites. The solution method has been used in order to achieve fine dispersion in thermoplastic and thermosetting matrices [29]. The melt blending or extrusion technique has also been recognized for significantly manufacturing polymer/graphene nanocomposites [62–64]. This method is simple and solvent free. Polymer and graphene are usually fed into an extruder. In this method, a high shear rate and temperature conditions are applied. The melt casting of nanocomposites may enhance nanofiller dispersion and nanocomposite properties [65,66]. In situ polymerization was found to be efficient for graphene dispersion and interaction with polymers [67]. In this method, monomers are polymerized in situ with graphene nanofiller [68]. Examples include polystyrene, polyaniline, polypyrrole, etc. [69–71].

### 3. EMI Shielding

Harmful electromagnetic fields have been continuously generated by electronic devices [72]. To protect the surroundings from harmful radiations, materials with excellent magnetic permeability properties have been found indispensable [73]. Traditionally, metal and alloys have been used as electromagnetic defensive shields. However, metals have key disadvantages of weight, formability, and corrosion, thereby, improvements are needed to attain commercial use. Consequently, the research has shifted towards polymer- and nanomaterial-based electromagnetic defense materials [74]. Polymeric nanocomposites have advantageous physical features in order to achieve efficacy of electromagnetic shields [75,76]. Figure 1 shows the EMI shielding mechanism. Three especially important mechanisms may lead to radiation effectiveness, i.e., the absorption of incident radiations, reflection of radiations, and multiple internal reflections.

In nanocomposites, the type of nanofiller, amount, and dispersion was found to be significant for superior shielding interference [77]. In this context, the electromagnetic shielding mechanism is investigated in the literature [78]. The shielding phenomenon was found to be comprised of reflections and multiple reflections [79]. The uniform nanocomposites have excellent radiation absorption properties, as compared to the randomly scattered nanoparticle-based nanomaterials. The complex shielding phenomenon is observed in the non-homogeneous nanocomposites [80–82]. Figure 2 displays the timeline of the step-wise adopting of carbon materials for radiation protection [73]. Carbon black was used to achieve a radiation defense during World War II. From 1941 to 1945, rubber filled with carbon black and Aluminum flakes were used to achieve an EMI SE of 15–20 dB in X-band [83]. Till the 1990s, graphite and carbon black were applied followed by the use of carbon nanotubes [84]. Subsequently, since 2010, graphene has been applied as an emergent shielding material [85]. EMI shielding nanocomposites have been efficiently used in technological industries such as the electronics, energy devices, sensors, engineering, automobile, aerospace, and biomedical fields [86,87].

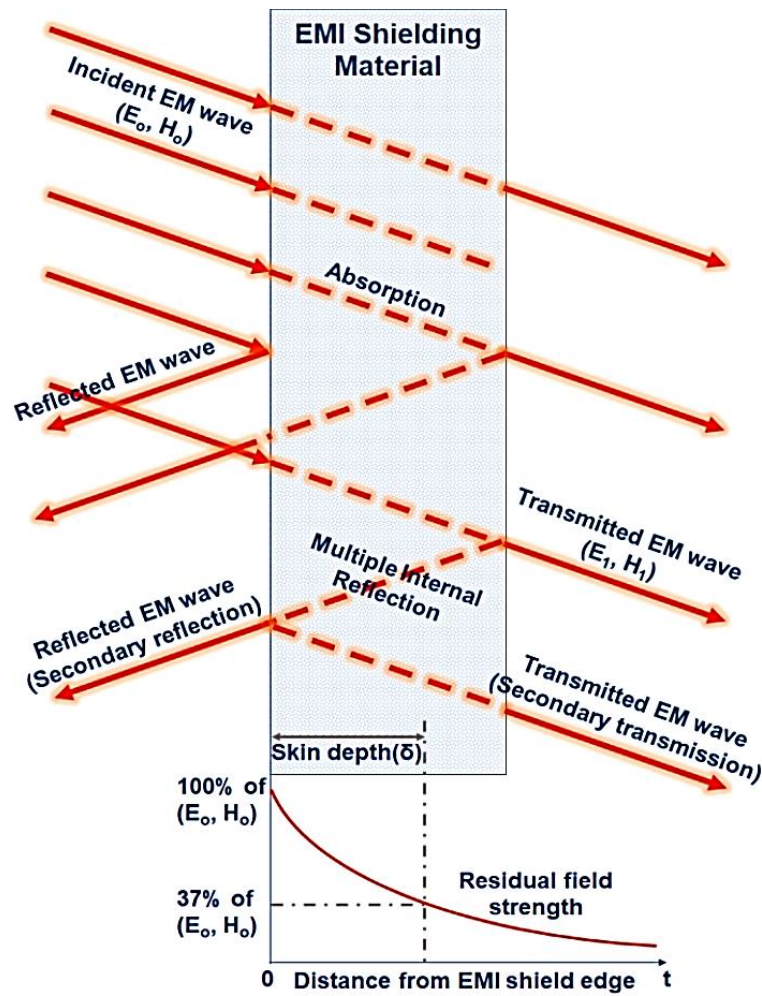


Figure 1. Schematic representation of EMI shielding mechanism [73]. Reproduced with permission from Elsevier.

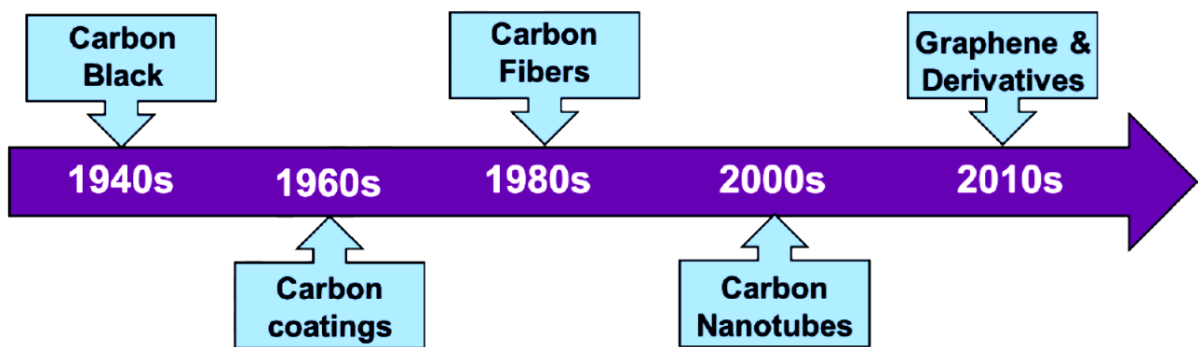


Figure 2. Historical background of the carbon material used in electromagnetic shielding applications [73]. Reproduced with permission from Elsevier.

The carbon nanoparticles were found to be effective in enhancing the radiation protection of polymeric nanomaterials [88]. Among these nanoparticles, graphene, graphene oxide, carbon nanofibers, carbon nanotube, carbon black, etc., have been recurrently used in order to achieve superior EMI shielding [89]. Magnetic nanoparticles and inorganic and metal nanoparticles have also been used to improve the radiation defense of the polymer-based nanocomposites [90,91]. The performance and efficiency of nanocomposite-based radiation shielding materials is found to be directly dependent upon an improved

nanofiller dispersion in the matrices for superior radiation absorption [92]. Moreover, the radiation shielding mechanism usually depends on a consistent network formation between polymers and nanoparticles, thereby enabling excellent electrical conduction [93]. Other superior nanocomposite properties are indispensable to attain high performance nanocomposite shields, including superior heat stability, strength, as well as anti-corrosion, for industrial applications [94].

#### 4. Graphene Nanocomposites for EMI Shielding

Electronic devices and equipment generate harmful electromagnetic fields for surroundings, living beings, and environments [95–97]. Consequently, not only the entire ecosystem is disturbed, but electronic device performance is also hindered. Consequently, polymer and nanocomposite materials have been developed for electromagnetic defense [98–100]. Conducting as well as non-conducting polymers were reinforced with nanocarbons and inorganic nanoparticles in order to achieve superior radiation shielding [101,102]. In this context, the nanocarbon nanofillers were found to be more effective to improve the EMI SE, compared with that of the inorganic nanoparticles. One major role of nanoparticles is to increase the electrical conductivity of polymers, thereby effecting the EMI shielding efficiency of nanocomposites [103–105]. Among carbon nanoparticles, graphene was found to be effective to develop radiation protection shields of polymeric nanocomposites [106,107].

Conducting polymer and graphene-based nanocomposites have the capability to improve radiation absorption and electromagnetic radiation shielding properties [108,109]. Advanced electronics, microelectronics, as well as optoelectronic devices, have been designed using polymer/graphene nanocomposites to achieve a strong EMI defense [110–112]. Polyaniline, polypyrrole, and polythiophene are often used as important conducting polymers. Polyaniline is the most frequently used conjugated polymer for EMI shielding. Several research efforts were performed on polyaniline- and graphene-based nanocomposites [113]. For example, a moderately high EMI SE of 20 dB has been reported for these nanocomposites [114]. Shen and researchers [115] fabricated polymer/graphene nanocomposite design for superior radiation shielding properties. The EMI dB of  $\geq 20$  dB was observed in the frequency range of 5.4 to 59.6 GHz. Superior electromagnetic interference shielding properties were achieved due to the high electrical conductivity and matrix-nanofiller associations. Khasim [116] and colleagues reported para-toluene sulphonic acid-doped polyaniline and graphene nanoplatelet-based nanocomposites. The para-toluene sulphonic acid-doped polyaniline/graphene nanoplatelet nanocomposite revealed excellent shielding efficiency of  $>95\%$  at 10 wt.% nanofiller addition. The material thickness was adjusted at  $\sim 1.5$  mm. The modified polyaniline and graphene nanoplatelets developed interconnecting network structures due to  $\pi$ - $\pi$  stacking, thereby enabling high electron mobilization, charge density, and radiation shielding properties. The doping of polyaniline also improved the electron conduction of polyaniline by many folds. Figure 3 displays the variations in electrical conductivity versus the changing frequency. High nanofiller contents possess more graphene nanoplatelet galleries for incorporating aniline monomers, thereby causing in situ polymer formation. Consequently, the electrical conductivity of the nanocomposites was improved with nanofiller loading. Figure 4 illustrates the influence of nanofiller on real and imaginary parts of the dielectric constant of radiation shielding material. Accordingly, the complex permittivity real part was increased from 18.4 to 23.2, and the complex permittivity imaginary part was improved from 14 to 21.8.

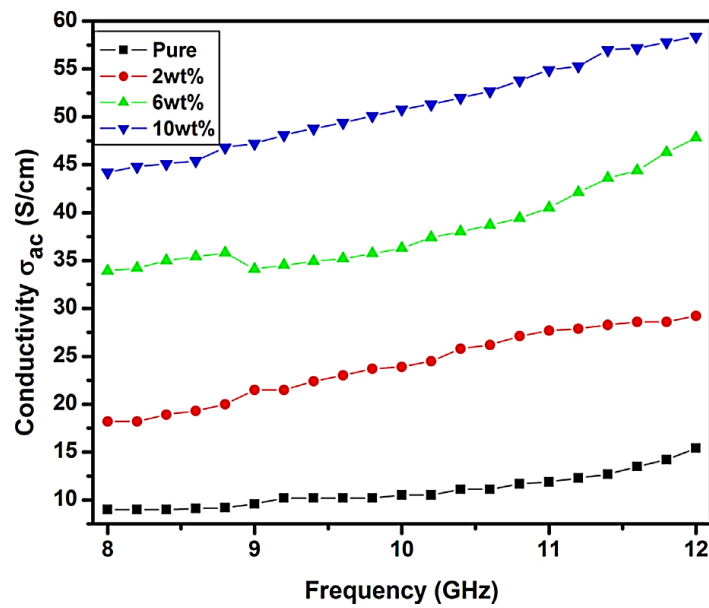


**Figure 3.** AC conductivity as a function of frequency for pure polyaniline (PANI) and polyaniline/graphene nanoplatelets (PANI-GRNPs) nanocomposites in X-band [116]. Reproduced with permission from Elsevier.

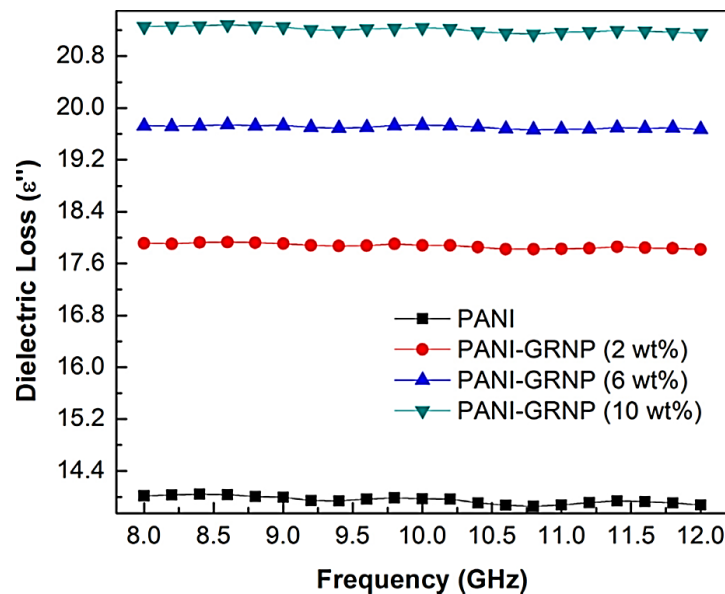


**Figure 4.** Variation of dielectric loss as a function of frequency for polyaniline (PANI) and polyaniline/graphene nanoplatelets (PANI-GRNPs) nanocomposites in X-band [116]. Reproduced with permission from Elsevier.

Polythiophene has also been applied to form EMI shielding materials due to superior electrical conductivity properties [117–119]. However, it is a less explored polymer than the polyaniline and polypyrrole matrices. The polythiophene-derived nanocomposites had an EMI shielding efficiency of ~44 dB, along with 99% absorption at 11.65 GHz. The EMI shielding efficiency of polythiophene-based materials was improved due to conducting components in the nanocomposite, thereby resisting the undesirable radiations [120]. Furthermore, the thickness, magnetic features, as well as the electrical permittivity/permeability of polythiophene based shields were considered especially significant factors [117]. The shielding mechanism was found to be dependent on the absorption of incident radiation via magnetic or electric dipole formation. Guo and co-workers [121] reported polythiophene/graphene

nanocomposites having excellent EMI shielding properties. In these nanocomposites, interactions and interface development among conducting polymer and graphene influenced the EMI shielding behavior of the resulting materials.

In addition to conjugated polymers, non-conducting materials have gained research interest in achieving high performance EMI shielding properties [122–124]. Especially, thermosets (such as epoxy resin) and a range of thermoplastics have been investigated for radiation shielding applications [125–127]. Hence, non-conducting polymers have been applied to enhance material properties using nanofillers [128]. In this context, nanofillers were indispensable to generate conductivity and shielding properties in the matrices. Wei et al. [129] developed poly(methyl methacrylate-butyl acrylate)- and poly(styrene-butyl acrylate)-based nanocomposites reinforced with sulfonated graphene nanofiller. The poly(methyl methacrylate-butyl acrylate)/sulfonated graphene nanosheets and poly(styrene-butyl acrylate)/sulfonated graphene nanosheets nanocomposites have  $\pi$ - $\pi$  stacking, thereby enabling a well-compatible interface. Transmission electron microscopy images of sulfonated graphene nanosheets, poly(methyl methacrylate-butyl acrylate)/sulfonated graphene nanosheets, and poly(styrene-butyl acrylate)/sulfonated graphene nanosheet nanocomposites are shown in Figure 5. The 3 wt.% nanofiller reinforcement was used in the nanocomposites. Neat sulfonated graphene nanosheets revealed a homogeneous structure, along with few micro-wrinkles. On the other hand, poly(methyl methacrylate-butyl acrylate) and poly(styrene-butyl acrylate) matrices can be seen coated on the sulfonated graphene nanosheet surface in the nanocomposite samples. The polymer layering on nanofiller nanosheets was attributed to  $\pi$ - $\pi$  stacking interactions and interface formation. Figure 6 demonstrates the EMI SE of a poly(styrene-butyl acrylate)/sulfonated graphene nanosheet nanocomposite reinforced with 25 wt.% nanofiller contents. The EMI SE was increased with the changing material thickness. The 0.05-mm-thick nanocomposite nanosheet caused an EMI SE of 21.5 dB (11.35–12.35 GHz). Consequently, increasing the shield thickness to 1.8 mm significantly improved the EMI SE, up to 80 dB.

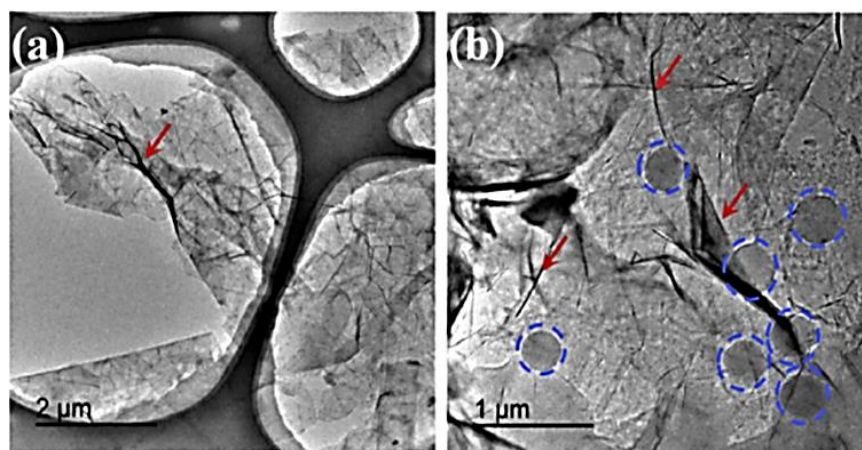


**Figure 5.** TEM images of (a) S-GNS; (b) P(St-BA)/S-GNS-3 wt.% nanocomposite latex [129]. S-GNS = sulfonated graphene nanosheets; P(MMA-BA) = poly(methyl methacrylate-butyl acrylate); P(St-BA) = poly(styrene-butyl acrylate); red arrows = wrinkled structure of graphene; blue dotted circles = latex particles. Reproduced with permission from Elsevier.

Hamidinejad and co-workers [130] investigated the design of a polyethylene/graphene nanoplatelet nanocomposite through an injection molding method. The nanocomposites were found suitable for EMI shielding. The inclusion of a graphene nanoplatelet in the matrix improved the interfacial interactions, thereby enhancing the particle dispersal. Consequently, a low percolation threshold and excellent electron conduction, as well as EMI SE, were observed. The electromagnetic shielding was observed due to multiple reflections in the dispersed graphene nanoplatelet nanocomposites. Accordingly, superior interfacial interactions between the polyethylene and graphene nanoplatelet improved the electrical

conductivity and dielectric properties, as well as the permittivity of the nanocomposites. Consequently, these effects enabled a considerably high EMI SE of 31.6 dB for 19 vol.% graphene nanoplatelet-filled nanocomposites.

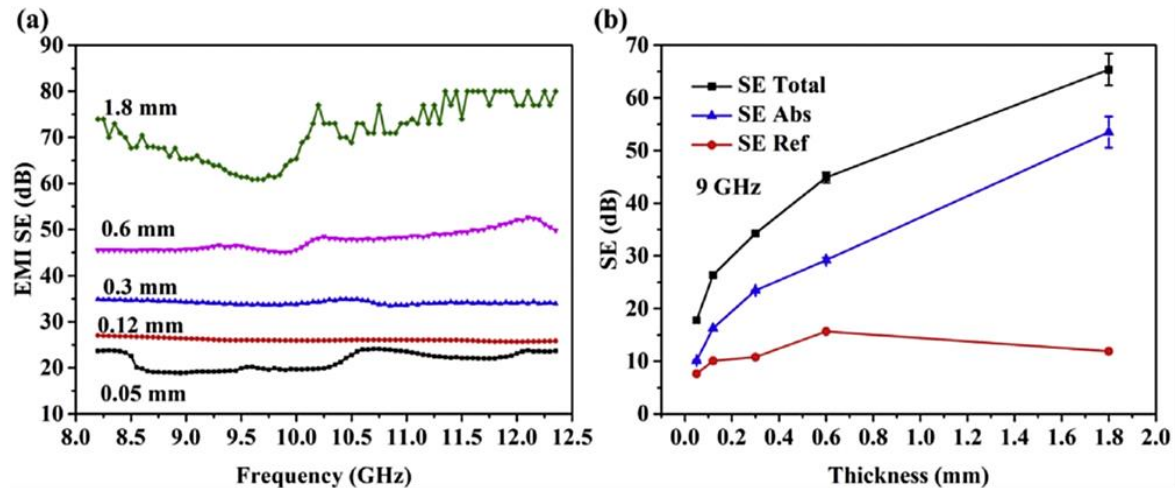


**Figure 6.** (a) EMI SE values of P(St-BA)/S-GNS-25 wt.% nanocomposites with different thickness; (b) SE Total,  $SE_{Abs}$ , and  $SE_{Ref}$  or various thickness at 9 GHz [129]. P(St-BA) = poly(styrene-butyl acrylate); S-GNS = sulfonated graphene nanosheet; EMI SE = electromagnetic interference shielding effectiveness. Reproduced with permission from Elsevier.

Anderson and co-workers [131] investigated epoxy/graphene nanoplatelet nanocomposites. Superior electrical conductivity, dielectric, and permittivity features of the nanocomposites were found to be dependent on the formation of a compatible interface and mutual interactions. These properties were studied using numerical solutions to Maxwell's equations. Moreover, interactions between the matrix and nanofiller directly affected the nanofiller dispersion. Superior nanofiller dispersion developed interfacial areas in the nanocomposite. Consequently, the EMI shielding properties of the ensuing nanocomposites were significantly enhanced.

Pavlou and colleagues [132] fabricated poly(methyl methacrylate) and graphene nanolaminate-derived nanocomposites. The mutual interactions and interface development improved the EMI SE of the nanocomposites. Figure 7 shows the radiation shielding effectiveness of the poly(methyl methacrylate) nanocomposite, with 0.33 vol.% graphene nanolaminates. The nanocomposite, developed with a 33  $\mu\text{m}$  thickness, gives rise to an EMI SE of 60 dB at a 2 THz frequency. According to the research, the enhancement in thickness shields enabled an excellent EMI SE of the nanocomposites. Consequently, the EMI SE was enhanced up to  $3 \times 10^5$  dB. Hence, the significantly high value of shielding effectiveness obtained was comparable to the metallic shields for radiation defense.

Lakshmi et al. [133] fabricated the poly(vinylidene fluoride) and graphene quantum dot-derived nanomaterials. Pristine poly(vinylidene fluoride) had an EMI SE of 0 dB, which considerably improved to 31 dB (at 8 GHz) in the poly(vinylidene fluoride)/graphene quantum dot nanocomposite. The radiation protection mechanism was found to be dependent upon the efficient reflection and absorption of radiation caused by the electrical charge flow at the compatible interface. Accordingly, a superior dielectric constant and EMI SE were observed due to fine graphene quantum dot dispersion. Table 1 presents poly(methyl methacrylate) [134], poly(dimethyl sulfoxide) [135,136], poly(vinylidene fluoride) [137], polyaniline, polyimide/polyaniline [138,139], polyurethane [140], epoxy [140], and graphene nanofiller-based systems for EMI SE performance. All these nanomaterial systems possess fine nanofiller dispersion and interface formation, thereby enabling excellent electrical conductivity and radiation shielding properties of the nanocomposites.

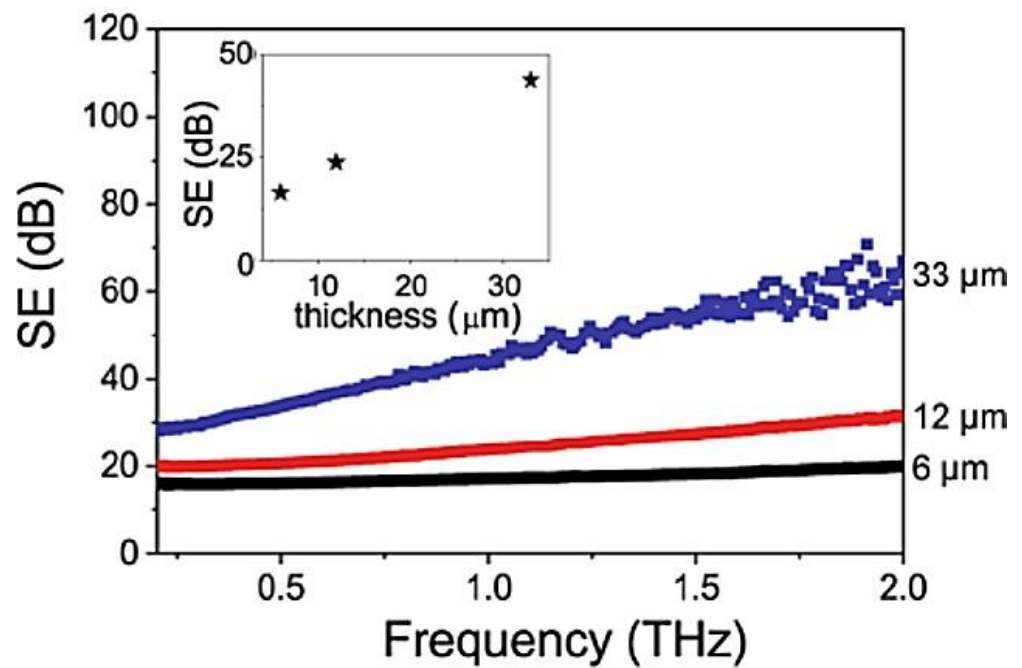


**Figure 7.** Shielding effectiveness of neat nanolaminate and filled with 0.33 vol.% graphene nanofiller [132]. Inset (stars) = shielding efficiency (SE) measured at 1 THz as a function of thickness; black line = reference data; red line = neat poly(methyl methacrylate); blue line = poly(methyl methacrylate) with 0.33% nanofiller. Reproduced with permission from Creative Commons CC BY.

**Table 1.** Electrical conductivity and electromagnetic interference shielding of graphene-derived nanocomposites.

Matrix	Nanofiller	Electrical Conductivity	Electromagnetic Interference Shielding (EMI SE) (dB)	Ref.
Polyaniline	Graphene	490.3 S cm <sup>-1</sup>	21.3	[138]
Polyimide/Polyaniline	Graphene	490.3 S cm <sup>-1</sup>	16.4	[134]
Polyimide/Polyaniline	Graphene/Fe <sub>3</sub> O <sub>4</sub>	2.5 S cm <sup>-1</sup>	32.4	[139]
Polyamide 6	Graphene	29.6 S·m <sup>-1</sup>	41.8	[141]
Polyurethane	Graphene	460.0 S cm <sup>-1</sup>	30.7	[140]
Poly(vinylidene fluoride)	Graphene	0.015 S cm <sup>-1</sup>	32.5	[137]
Poly(methyl methacrylate)	Graphene	0.013 S cm <sup>-1</sup>	47.5	[134]
Poly(methyl methacrylate)	Reduced graphene	0.0292 S cm <sup>-1</sup>	43.4	[134]
Poly(methyl methacrylate)	Reduced graphene	0.0015 S cm <sup>-1</sup>	26.2	[134]
Poly(dimethyl sulfoxide)	Graphene/Fe <sub>3</sub> O <sub>4</sub>	25 S cm <sup>-1</sup>	249	[135]
Poly(dimethyl sulfoxide)	Graphene	0.20 S cm <sup>-1</sup>	54.4	[136]
Epoxy	Reduced graphene oxide	3.87 S cm <sup>-1</sup>	55.0	[140]

### 5. Interfacial Interactions in Polymer/Graphene Nanocomposites

Due to superior electron conduction properties, carbon nanoparticles such as graphene [142,143] and carbon nanotube [144,145] have been applied as nanofillers in EMI shielding materials. These nanofillers can easily form interconnecting networks in the polymer matrices [146–148]. In addition, carbon nanofillers have fine dispersions in the matrices due to interface formation, thereby enabling high electrical conductivity and radiation shielding properties [149]. The formation of a compatible interface between

the polymer and graphene was found to be useful for enhancing radiation protection characteristics [150]. Covalent interactions between the matrix and nanofiller play an especially important role in the formation of compatible nanocomposites [151]. In addition, non-covalent interactions, such as  $\pi$ - $\pi$  stacking and van der Waals forces, have also been observed [152]. Due to the  $sp^2$  hybridized nanostructure, graphene developed  $\pi$ - $\pi$  stacking interactions with the polymers [153]. These interactions improved the electron conduction, radiation shielding, mechanical robustness, and heat stability properties. Ma and co-workers [154] reported covalently linked polymer- and graphene-derived nanomaterials. The covalent linking as well as the aromatic stacking interactions enabled compatible interface formations, thereby improving the mechanical characteristics. Adding a graphene nanofiller in polymer also improved Young's modulus and fracture toughness by 84.6% and 47.7%, respectively. Shen and researchers [155] developed epoxy/graphene oxide nanocomposites and reinforced them in the polycarbonate matrix. The mutual interactions, interface formation, and effect on the nanocomposite properties have been explored. Interfacial interactions between polymer and nanofiller have been considered important for the formation of strong covalent bonding or crosslinking. Figure 8 demonstrates covalent linking among the diglycidyl ether of bisphenol A and graphene oxide through a grafting to approach. The covalent bonding was established between the epoxide functionalities of epoxy resin and the carboxylic acid groups of graphene oxide, thereby enabling strong interface bonding. The formation of a polycarbonate/epoxy/graphene oxide nanocomposite is given in Figure 9a. The epoxide and hydroxyl groups of epoxy/graphene oxide developed covalent linking with the polycarbonate matrix. Consequently, the covalent linking of epoxy to graphene oxide and polycarbonate gives rise to the formation of a well-compatible interface and interfacial interactions. Figure 9b–d presents scanning electron microscopy micrographs of a polycarbonate/epoxy/graphene oxide nanocomposite. Graphene oxide strongly interacted with the polymer matrix through interactions for fine dispersion properties. Graphene oxide aggregation was supposed to prevent the interfacial covalent interactions between polymers and graphene oxide. Accordingly, the significance of interfacial interactions in polymer/graphene or graphene oxide has been analyzed.

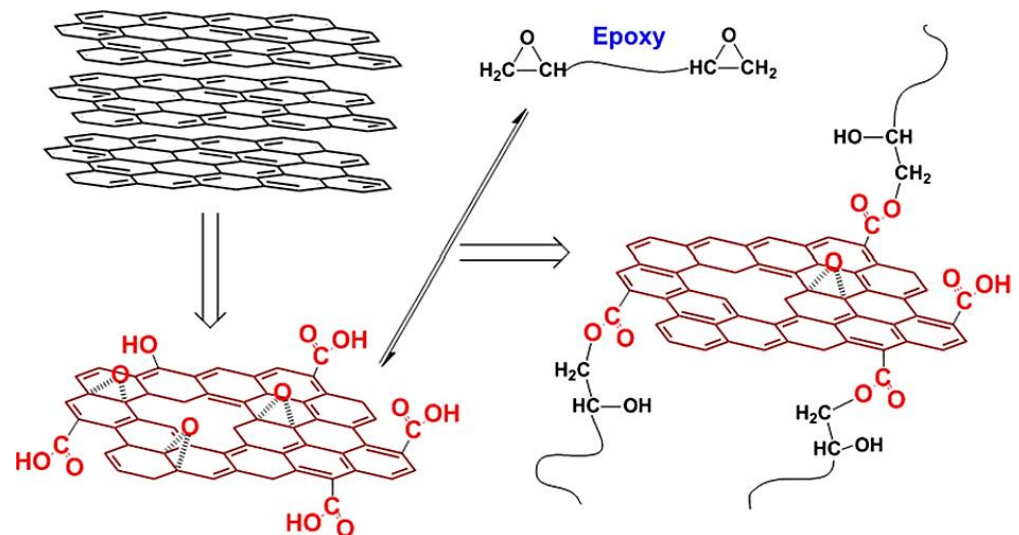


**Figure 8.** Schematic of epoxy/graphene oxide synthesis [155]. Here, arrows show reversible reaction between epoxy and carboxylic acid groups; oxygen functional groups on graphene nanosheet are colored red. Reproduced with permission from Elsevier.

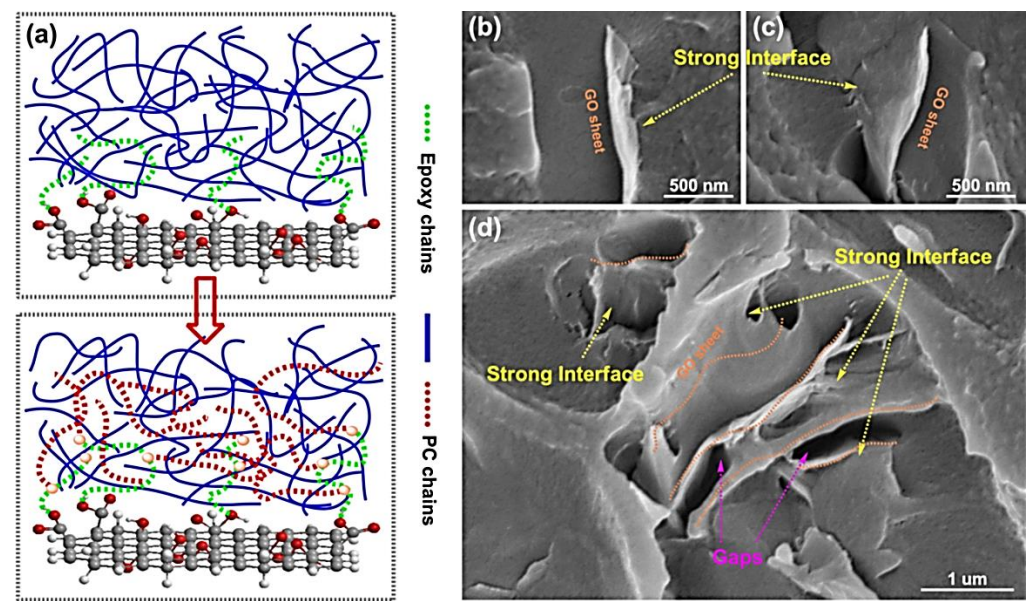


**Figure 9.** (a) Schematic drawing of covalent bonds between epoxy/graphene oxide and polycarbonate (PC) matrix; a broad red arrow shows mixing of epoxy and polycarbonate chains; graphene nanosheet with gray balls = carbon; red balls = oxygen; white balls = hydrogen atoms; (b–d) scanning electron microscopy images of polycarbonate/epoxy/graphene oxide nanocomposite showing fracture surface topography [155]. Reproduced with permission from Elsevier.

## 6. Value of Graphene Nanocomposites in EMI Shielding

Continuous research gives rise to the technologically advanced composite materials [156]. Consequently, polymers and nanocomposites have been used to attain EMI SE performance [157]. These polymeric materials and nanocomposites revealed fine morphology, electrical conductivity, dielectric/magnetic features, mechanical strength, heat stability, as well as corrosion resistance characteristics. The polymers were reinforced with carbon nanofiller-like graphene, graphene derivatives, and carbon nanotubes to improve the EMI shielding efficiency [158]. However, metal nanoparticles and inorganic nanofillers have also been reported as polymer reinforcements for EMI SE features [159,160]. In this context, it was essential to study and understand the mechanism of radiation shielding materials [161].

As discussed in the above sections, both conjugated and non-conjugated polymers have been used to form nanocomposites with graphene and graphene derivatives. The conjugated polymers (polyaniline, polythiophene, etc.), thermosets (epoxy), and thermoplastic polymers (polyethylene, poly(methyl methacrylate), etc.) have been used as matrices for graphene nanofillers, thereby forming polymer/graphene nanocomposites [162]. The EMI shielding properties of graphene-derived nanocomposites were found to be dependent on the material design, electrical conductivity, matrix-nanofiller interactions, as well as the fabrication method and parameters [163]. In high performance nanocomposites, polymer and graphene together form an interconnected network, thereby improving the electron mobility and radiation shielding [164]. The cooperative effect of graphene and polymer matrices enabled high performance shielding materials. Functional graphene or modified graphene usually has excellent compatibility with the polymer matrices. Graphene oxide is a modified form of graphene effectively used with polymers to achieve improved EMI shielding properties. The radiation defense can also be enhanced by using efficient polymer-based designs, as well as through suitable synthesis approaches. Using modified polymer and nanocomposite can improve the overall material performance. Furthermore, the performances of polymer/graphene nanomaterials in EMI devices can be improved through altering the design and processing parameters of these materials [165].

The future of graphene-based materials depends upon understanding the EMI mechanism, design and fabrication strategies, nanofiller modification, nanofiller amount, nanoparticle dispersion, interactions, and morphological properties [166]. Consequently, controlling these parameters can enable improved electromagnetic absorption features of the advanced polymer- and graphene-based nanomaterials. The contents and dispersion of graphene and graphene derivatives were found to be crucial to form homogeneous nanocomposites enabling excellent conductivity and EMI shielding properties. Fine graphene dispersion was found to be indispensable to attain advanced radiation defense nanomaterials. Using two or more polymer blends can also cause improved EMI SE performance. For example, blends of conducting polymers with thermosets or thermoplastics have been applied [167]. Another important factor is the adjustment of the thickness of radiation shields for superior electromagnetic protection features [168]. In this context, the formation of three-dimensional graphene-based nanoarchitectures can also enhance electron transportation, radiation defense, and other physical properties of the nanostructures [169]. In the future, advanced systems can be developed using eco-polymers and graphene nanofillers, thereby forming environmentally friendly EMI shielding equipment [170]. In this manner, highly efficient future polymer- and graphene-derived nanocomposites can be used for superior electromagnetic shielding effects [171].

## 7. Conclusions

In this literature overview, polymer- and graphene-derived nanocomposites have been discussed, ranging from their EMI shielding phenomenon to fundamentals, and radiation shielding effectiveness. The polymer- and nanocarbon-based nanomaterials were found to be excellent alternatives to metal-based radiation shields due to their low density, fine durability, superior electrical conductivity, as well as their high radiation protection. Both conducting and non-conducting matrices have been applied along with graphene- and graphene derivative-based nanofillers. Furthermore, graphene-derived nanocomposites possess fine processing, controllable thickness, and superior radiation absorption properties. The polymer/graphene nanocomposites have been effectively utilized due to their low price, excellent electrical conductivity, dielectric, permittivity, as well as their EMI SE features. In this context, it is especially important to design a polymer/graphene interface to improve the EMI shielding effectiveness. High performance nanocomposites were produced due to the synergistic effects of graphene, graphene oxide, and modified graphene with polymers and their mutual interactions. Moreover, significant factors governing the electric, magnetic and shielding properties include the nanofiller functionality, concentration, dispersion, overall material morphology, along with physical properties (electrical, thermal, mechanical, corrosion). The synchronization between the conductivity and permittivity of nanocomposites was found to be useful to enhance the shielding properties. Hence, this article highlights the research and developments of polymer- and graphene-based nanocomposites towards advanced EMI shielding materials.

**Author Contributions:** Conceptualization, A.K.; data curation, A.K.; writing of original draft preparation, A.K.; Review and editing, A.K., I.A., T.Z., O.A., K.H.I., M.H.E. and T.D.L. All authors have read and agreed to the published version of the manuscript.

**Funding:** This work was supported and funded by the Deanship of Scientific Research at Imam Mohammad Ibn Saud Islamic University (IMSIU) (grant number IMSIU-RG23033).

**Data Availability Statement:** Not applicable.

**Acknowledgments:** The authors appreciate the Deanship of Scientific Research at Imam Mohammad Ibn Saud Islamic University (IMSIU) for supporting and supervising this project.

**Conflicts of Interest:** The authors declare no conflict of interest.

## References

1. Bol-Arreba, A.; Ayala, I.G.; Cordero, N.A. Graphene Formation through Spontaneous Exfoliation of Graphite by Chlorosulfonic Acid: A DFT Study. *Micro* **2023**, *3*, 143–155. [[CrossRef](#)]
2. Goustouridis, D.; Raptis, I.; Mpatzaka, T.; Fournari, S.; Zisis, G.; Petrou, P.; Beltsios, K.G. Non-Destructive Characterization of Selected Types of Films and Other Layers via White Light Reflectance Spectroscopy (WLRS). *Micro* **2022**, *2*, 495–507. [[CrossRef](#)]
3. Lucido, M. Helmholtz–Galerkin Regularizing Technique for the Analysis of the THz-Range Surface-Plasmon-Mode Resonances of a Graphene Microdisk Stack. *Micro* **2022**, *2*, 295–312. [[CrossRef](#)]
4. Kausar, A.; Ahmad, I.; Aldaghri, O.; Ibnaouf, K.H.; Eisa, M. Shape Memory Graphene Nanocomposites—Fundamentals, Properties, and Significance. *Processes* **2023**, *11*, 1171. [[CrossRef](#)]
5. Xu, F.; Gao, M.; Wang, H.; Liu, H.; Yan, F.; Zhao, H.; Yao, Q. Polymer-based graphene composite molding: A review. *RSC Adv.* **2023**, *13*, 2538–2551. [[CrossRef](#)]
6. Zhang, H.; Lin, S. Research Progress with Membrane Shielding Materials for Electromagnetic/Radiation Contamination. *Membranes* **2023**, *13*, 315. [[CrossRef](#)]
7. Wu, H.; Wu, G.; Zhao, B. Special issue on electromagnetic wave absorbing materials. *J. Mater. Sci. Mater. Electron.* **2021**, *32*, 25561. [[CrossRef](#)]
8. Gao, A.; Xu, D.; Li, C.; Wang, Y.; Xu, L. Interfacial reactions in graphene oxide/polyacrylonitrile composite films. *Compos. Interfaces* **2021**, *28*, 159–173. [[CrossRef](#)]
9. Cao, L.; Liu, Y.; Zhang, D. Effect of esterification crosslinking on interfacial heat transfer between graphene and phase change material. *Compos. Interfaces* **2020**, *28*, 1121–1135. [[CrossRef](#)]
10. Hui, J.; Ren, P.-G.; Sun, Z.-F.; Ren, F.; Xu, L.; Zhang, Z.-P.; Ji, X. Influences of interfacial adhesion on gas barrier property of functionalized graphene oxide/ultra-high-molecular-weight polyethylene composites with segregated structure. *Compos. Interfaces* **2017**, *24*, 729–741. [[CrossRef](#)]
11. Novoselov, K.S.; Fal, V.; Colombo, L.; Gellert, P.; Schwab, M.; Kim, K. A roadmap for graphene. *Nature* **2012**, *490*, 192–200. [[CrossRef](#)]
12. Usachov, D.; Adamchuk, V.; Haberer, D.; Grüneis, A.; Sachdev, H.; Preobrajenski, A.; Laubschat, C.; Vyalikh, D. Quasifreestanding single-layer hexagonal boron nitride as a substrate for graphene synthesis. *Phys. Rev. B* **2010**, *82*, 075415. [[CrossRef](#)]
13. Gao, Y.; Zhang, Y.; Chen, P.; Li, Y.; Liu, M.; Gao, T.; Ma, D.; Chen, Y.; Cheng, Z.; Qiu, X. Toward single-layer uniform hexagonal boron nitride–graphene patchworks with zigzag linking edges. *Nano Lett.* **2013**, *13*, 3439–3443. [[CrossRef](#)]
14. Girit, Ç.Ö.; Meyer, J.C.; Erni, R.; Rossell, M.D.; Kisielowski, C.; Yang, L.; Park, C.-H.; Crommie, M.; Cohen, M.L.; Louie, S.G. Graphene at the edge: Stability and dynamics. *Science* **2009**, *323*, 1705–1708. [[CrossRef](#)]
15. Gómez-Navarro, C.; Meyer, J.C.; Sundaram, R.S.; Chuvilin, A.; Kurasch, S.; Burghard, M.; Kern, K.; Kaiser, U. Atomic structure of reduced graphene oxide. *Nano Lett.* **2010**, *10*, 1144–1148. [[CrossRef](#)]
16. Huang, P.Y.; Ruiz-Vargas, C.S.; Van Der Zande, A.M.; Whitney, W.S.; Levendorf, M.P.; Kevek, J.W.; Garg, S.; Alden, J.S.; Hustedt, C.J.; Zhu, Y. Grains and grain boundaries in single-layer graphene atomic patchwork quilts. *Nature* **2011**, *469*, 389–392. [[CrossRef](#)]
17. Berger, C.; Song, Z.; Li, X.; Wu, X.; Brown, N.; Naud, C.; Mayou, D.; Li, T.; Hass, J.; Marchenkov, A.N. Electronic confinement and coherence in patterned epitaxial graphene. *Science* **2006**, *312*, 1191–1196. [[CrossRef](#)]
18. Avouris, P.; Dimitrakopoulos, C. Graphene: Synthesis and applications. *Mater. Today* **2012**, *15*, 86–97. [[CrossRef](#)]
19. Tour, J.M. Top-down versus bottom-up fabrication of graphene-based electronics. *Chem. Mater.* **2014**, *26*, 163–171. [[CrossRef](#)]
20. Huang, Y.-H.; Bao, Q.; Duh, J.-G.; Chang, C.-T. Top-down dispersion meets bottom-up synthesis: Merging ultranano silicon and graphene nanosheets for superior hybrid anodes for lithium-ion batteries. *J. Mater. Chem. A* **2016**, *4*, 9986–9997. [[CrossRef](#)]
21. Zhang, Z.; Fraser, A.; Ye, S.; Merle, G.; Barralet, J. Top-down bottom-up graphene synthesis. *Nano Futures* **2019**, *3*, 042003. [[CrossRef](#)]
22. Wei, C.; Negishi, R.; Ogawa, Y.; Akabori, M.; Taniyasu, Y.; Kobayashi, Y. Turbostratic multilayer graphene synthesis on CVD graphene template toward improving electrical performance. *Jpn. J. Appl. Phys.* **2019**, *58*, S11B04. [[CrossRef](#)]
23. Cabrero-Vilatela, A.; Weatherup, R.S.; Braeuninger-Weimer, P.; Caneva, S.; Hofmann, S. Towards a general growth model for graphene CVD on transition metal catalysts. *Nanoscale* **2016**, *8*, 2149–2158. [[CrossRef](#)]
24. Kim, K.S.; Zhao, Y.; Jang, H.; Lee, S.Y.; Kim, J.M.; Kim, K.S.; Ahn, J.-H.; Kim, P.; Choi, J.-Y.; Hong, B.H. Large-scale pattern growth of graphene films for stretchable transparent electrodes. *Nature* **2009**, *457*, 706–710. [[CrossRef](#)]
25. Wang, M.; Jang, S.K.; Jang, W.J.; Kim, M.; Park, S.Y.; Kim, S.W.; Kahng, S.J.; Choi, J.Y.; Ruoff, R.S.; Song, Y.J. A Platform for Large-Scale Graphene Electronics—CVD Growth of Single-Layer Graphene on CVD-Grown Hexagonal Boron Nitride. *Adv. Mater.* **2013**, *25*, 2746–2752. [[CrossRef](#)]
26. Liang, J.; Li, L.; Tong, K.; Ren, Z.; Hu, W.; Niu, X.; Chen, Y.; Pei, Q. Silver nanowire percolation network soldered with graphene oxide at room temperature and its application for fully stretchable polymer light-emitting diodes. *ACS Nano* **2014**, *8*, 1590–1600. [[CrossRef](#)] [[PubMed](#)]
27. Narayanam, P.K.; Botcha, V.D.; Ghosh, M.; Major, S.S. Growth and Photocatalytic Behaviour of Transparent Reduced GO-ZnO Nanocomposite Sheets. *Nanotechnology* **2019**, *30*, 485601. [[CrossRef](#)]
28. Kausar, A. Potential of polymer/graphene nanocomposite in electronics. *Am. J. Nanosci. Nanotechnol. Res.* **2018**, *6*, 55–63.
29. Hu, K.; Kulkarni, D.D.; Choi, I.; Tsukruk, V.V. Graphene-polymer nanocomposites for structural and functional applications. *Prog. Polym. Sci.* **2014**, *39*, 1934–1972. [[CrossRef](#)]

30. Zandiatashbar, A.; Lee, G.-H.; An, S.J.; Lee, S.; Mathew, N.; Terrones, M.; Hayashi, T.; Picu, C.R.; Hone, J.; Koratkar, N. Effect of defects on the intrinsic strength and stiffness of graphene. *Nat. Commun.* **2014**, *5*, 3186. [[CrossRef](#)] [[PubMed](#)]
31. Yang, S.-T.; Chang, Y.; Wang, H.; Liu, G.; Chen, S.; Wang, Y.; Liu, Y.; Cao, A. Folding/aggregation of graphene oxide and its application in Cu<sup>2+</sup> removal. *J. Colloid Interface Sci.* **2010**, *351*, 122–127. [[CrossRef](#)]
32. Wang, W.-N.; Jiang, Y.; Biswas, P. Evaporation-induced crumpling of graphene oxide nanosheets in aerosolized droplets: Confinement force relationship. *J. Phys. Chem. Lett.* **2012**, *3*, 3228–3233. [[CrossRef](#)] [[PubMed](#)]
33. Zhou, Q.; Xia, G.; Du, M.; Lu, Y.; Xu, H. Scotch-tape-like exfoliation effect of graphene quantum dots for efficient preparation of graphene nanosheets in water. *Appl. Surf. Sci.* **2019**, *483*, 52–59. [[CrossRef](#)]
34. Mohan, V.B.; Lau, K.-T.; Hui, D.; Bhattacharyya, D. Graphene-based materials and their composites: A review on production, applications and product limitations. *Compos. Part B Eng.* **2018**, *142*, 200–220. [[CrossRef](#)]
35. Pei, S.; Cheng, H.-M. The reduction of graphene oxide. *Carbon* **2012**, *50*, 3210–3228. [[CrossRef](#)]
36. Lonkar, S.P.; Deshmukh, Y.S.; Abdala, A.A. Recent advances in chemical modifications of graphene. *Nano Res.* **2015**, *8*, 1039–1074. [[CrossRef](#)]
37. Wang, Y.; Yang, C.; Mai, Y.-W.; Zhang, Y. Effect of non-covalent functionalisation on thermal and mechanical properties of graphene-polymer nanocomposites. *Carbon* **2016**, *102*, 311–318. [[CrossRef](#)]
38. Criado, A.; Melchionna, M.; Marchesan, S.; Prato, M. The covalent functionalization of graphene on substrates. *Angew. Chem. Int. Ed.* **2015**, *54*, 10734–10750. [[CrossRef](#)]
39. Sun, L.; Wang, L.; Tian, C.; Tan, T.; Xie, Y.; Shi, K.; Li, M.; Fu, H. Nitrogen-doped graphene with high nitrogen level via a one-step hydrothermal reaction of graphene oxide with urea for superior capacitive energy storage. *Rsc. Adv.* **2012**, *2*, 4498–4506. [[CrossRef](#)]
40. Zhou, D.; Cheng, Q.-Y.; Han, B.-H. Solvothermal synthesis of homogeneous graphene dispersion with high concentration. *Carbon* **2011**, *49*, 3920–3927. [[CrossRef](#)]
41. Raccichini, R.; Varzi, A.; Passerini, S.; Scrosati, B. The role of graphene for electrochemical energy storage. *Nat. Mater.* **2015**, *14*, 271–279. [[CrossRef](#)]
42. Cui, C.; Huang, J.; Huang, J.; Chen, G. Size separation of mechanically exfoliated graphene sheets by electrophoresis. *Electrochim. Acta* **2017**, *258*, 793–799. [[CrossRef](#)]
43. Garlow, J.A.; Barrett, L.K.; Wu, L.; Kisslinger, K.; Zhu, Y.; Pulecio, J.F. Large-area growth of turbostratic graphene on Ni (111) via physical vapor deposition. *Sci. Rep.* **2016**, *6*, 19804. [[CrossRef](#)]
44. Nanjundappa, V.; Ramakrishna, T.; Kempahanumakkagari, S.; Prakash, H.; Praveen, B. Efficient strategies to produce Graphene and functionalized graphene materials: A review. *Appl. Surf. Sci. Adv.* **2023**, *14*, 100386.
45. Fang, L.; Xue, L.; Yang, P.; Li, X.; Wang, Z. A Facile Route to 4-Polyfluoroarylquinolin-2 (1 H)-ones and 4-Polyfluoroarylcoumarins via C–H Bond Activation. *Chem. Lett.* **2017**, *46*, 1223–1226. [[CrossRef](#)]
46. Eigler, S.; Hirsch, A. Chemistry with graphene and graphene oxide—Challenges for synthetic chemists. *Angew. Chem. Int. Ed.* **2014**, *53*, 7720–7738. [[CrossRef](#)]
47. Mao, S.; Wen, Z.; Kim, H.; Lu, G.; Hurley, P.; Chen, J. A general approach to one-pot fabrication of crumpled graphene-based nanohybrids for energy applications. *ACS Nano* **2012**, *6*, 7505–7513. [[CrossRef](#)]
48. Ebrahimi Naghani, M.; Neghabi, M.; Zadsar, M.; Abbastabar Ahangar, H. Synthesis and characterization of linear/nonlinear optical properties of graphene oxide and reduced graphene oxide-based zinc oxide nanocomposite. *Sci. Rep.* **2023**, *13*, 1496. [[CrossRef](#)]
49. Brodie, B.C. XIII. On the atomic weight of graphite. *Philos. Trans. R. Soc. Lond.* **1859**, *149*, 249–259.
50. Feicht, P.; Biskupek, J.; Gorelik, T.E.; Renner, J.; Halbig, C.E.; Maranska, M.; Puchtler, F.; Kaiser, U.; Eigler, S. Brodie’s or Hummers’ method: Oxidation conditions determine the structure of graphene oxide. *Chem. A Eur. J.* **2019**, *25*, 8955–8959. [[CrossRef](#)]
51. Sajeev, V.; Rane, S.; Ghosh, D.; Acharyya, N.; Roy Choudhury, P.; Mukherjee, A.; Roy Chowdhury, D. Terahertz sensing of reduced graphene oxide nanosheets using sub-wavelength dipole cavities. *Sci. Rep.* **2023**, *13*, 12374. [[CrossRef](#)] [[PubMed](#)]
52. Lee, H.; Lee, K.S. Interlayer Distance Controlled Graphene, Supercapacitor and Method of Producing the Same. Google Patents US20150103469A1, 26 February 2019.
53. Ke, Q.; Wang, J. Graphene-based materials for supercapacitor electrodes—A review. *J. Mater.* **2016**, *2*, 37–54. [[CrossRef](#)]
54. Shen, X.J.; Zeng, X.L.; Dang, C.Y. Graphene Composites. In *Handbook of Graphene Set*; Scrivener Publishing LLC: Beverly, MA, USA, 2019; Volume 1, pp. 1–25.
55. Han, J.T.; Jeong, B.H.; Seo, S.H.; Roh, K.C.; Kim, S.; Choi, S.; Woo, J.S.; Kim, H.Y.; Jang, J.I.; Shin, D.-C. Dispersant-free conducting pastes for flexible and printed nanocarbon electrodes. *Nat. Commun.* **2013**, *4*, 2491. [[CrossRef](#)]
56. Han, J.T.; Jang, J.I.; Cho, J.Y.; Hwang, J.Y.; Woo, J.S.; Jeong, H.J.; Jeong, S.Y.; Seo, S.H.; Lee, G.-W. Synthesis of nanobelt-like 1-dimensional silver/nanocarbon hybrid materials for flexible and wearable electronics. *Sci. Rep.* **2017**, *7*, 4931. [[CrossRef](#)]
57. Panwar, N.; Soehartono, A.M.; Chan, K.K.; Zeng, S.; Xu, G.; Qu, J.; Coquet, P.; Yong, K.-T.; Chen, X. Nanocarbons for biology and medicine: Sensing, imaging, and drug delivery. *Chem. Rev.* **2019**, *119*, 9559–9656. [[CrossRef](#)]
58. Freund, P.; Senkovska, I.; Kaskel, S. Switchable conductive MOF–nanocarbon composite coatings as threshold sensing architectures. *ACS Appl. Mater. Interfaces* **2017**, *9*, 43782–43789. [[CrossRef](#)]
59. Tang, C.; Titirici, M.-M.; Zhang, Q. A review of nanocarbons in energy electrocatalysis: Multifunctional substrates and highly active sites. *J. Energy Chem.* **2017**, *26*, 1077–1093. [[CrossRef](#)]

60. Yanik, M.O.; Yigit, E.A.; Akansu, Y.E.; Sahmetlioglu, E. Magnetic conductive polymer-graphene nanocomposites based supercapacitors for energy storage. *Energy* **2017**, *138*, 883–889. [[CrossRef](#)]
61. Ganguly, S. Preparation/processing of polymer-graphene composites by different techniques. In *Polymer Nanocomposites Containing Graphene*; Elsevier: Amsterdam, The Netherlands, 2022; pp. 45–74.
62. Sadeghi, A.; Moeini, R.; Yeganeh, J.K. Highly conductive PP/PET polymer blends with high electromagnetic interference shielding performances in the presence of thermally reduced graphene nanosheets prepared through melt compounding. *Polym. Compos.* **2019**, *40*, E1461–E1469. [[CrossRef](#)]
63. Gill, Y.Q.; Ehsan, H.; Mehmood, U.; Irfan, M.S.; Saeed, F. A novel two-step melt blending method to prepare nano-silicized-silica reinforced crosslinked polyethylene (XLPE) nanocomposites. *Polym. Bull.* **2022**, *79*, 10077–10093. [[CrossRef](#)]
64. Sanes, J.; Sánchez, C.; Pamies, R.; Avilés, M.-D.; Bermúdez, M.-D. Extrusion of polymer nanocomposites with graphene and graphene derivative nanofillers: An overview of recent developments. *Materials* **2020**, *13*, 549. [[CrossRef](#)] [[PubMed](#)]
65. Tan, B.; Thomas, N.L. A review of the water barrier properties of polymer/clay and polymer/graphene nanocomposites. *J. Membr. Sci.* **2016**, *514*, 595–612. [[CrossRef](#)]
66. Kausar, A. In-situ modified graphene reinforced polyamide 1010/poly (ether amide): Mechanical, thermal, and barrier properties. *Mater. Res. Innov.* **2019**, *23*, 191–199. [[CrossRef](#)]
67. Owji, E.; Ostovari, F.; Keshavarz, A. Influence of the chemical structure of diisocyanate on the electrical and thermal properties of in situ polymerized polyurethane–graphene composite films. *Phys. Chem. Chem. Phys.* **2022**, *24*, 28564–28576. [[CrossRef](#)]
68. Itapu, B.M.; Jayatissa, A.H. A review in graphene/polymer composites. *Chem. Sci. Int. J.* **2018**, *23*, 1–16. [[CrossRef](#)]
69. Lu, Y.; Wang, X.; Chen, D.; Chen, G. Polystyrene/graphene composite electrode fabricated by in situ polymerization for capillary electrophoretic determination of bioactive constituents in *Herba Houttuyniae*. *Electrophoresis* **2011**, *32*, 1906–1912. [[CrossRef](#)] [[PubMed](#)]
70. Montaina, L.; Carcione, R.; Pescosolido, F.; Montalto, M.; Battistoni, S.; Tamburri, E. Three-dimensional-printed polyethylene glycol diacrylate-polyaniline composites by in situ aniline photopolymerization: An innovative biomaterial for electrocardiogram monitoring systems. *ACS Appl. Electron. Mater.* **2023**, *5*, 164–172. [[CrossRef](#)]
71. Yang, X.; Zhang, Z.; Xiang, Y.; Sun, Q.; Xia, Y.; Xiong, Z. Superior Enhancement of the UHMWPE Fiber/Epoxy Interface through the Combination of Plasma Treatment and Polypyrrole In-Situ Grown Fibers. *Polymers* **2023**, *15*, 2265. [[CrossRef](#)]
72. Kaczor-Urbanowicz, K.E.; Martín Carreras-Presas, C.; Kaczor, T.; Tu, M.; Wei, F.; Garcia-Godoy, F.; Wong, D.T. Emerging technologies for salivaomics in cancer detection. *J. Cell. Mol. Med.* **2017**, *21*, 640–647. [[CrossRef](#)] [[PubMed](#)]
73. Wang, C.; Murugadoss, V.; Kong, J.; He, Z.; Mai, X.; Shao, Q.; Chen, Y.; Guo, L.; Liu, C.; Angaiah, S. Overview of carbon nanostructures and nanocomposites for electromagnetic wave shielding. *Carbon* **2018**, *140*, 696–733. [[CrossRef](#)]
74. González, M.; Pozuelo, J.; Baselga, J. Electromagnetic shielding materials in GHz range. *Chem. Rec.* **2018**, *18*, 1000–1009. [[CrossRef](#)] [[PubMed](#)]
75. Gupta, S.; Sharma, S.K.; Pradhan, D.; Tai, N.-H. Ultra-light 3D reduced graphene oxide aerogels decorated with cobalt ferrite and zinc oxide perform excellent electromagnetic interference shielding effectiveness. *Compos. Part A Appl. Sci. Manuf.* **2019**, *123*, 232–241. [[CrossRef](#)]
76. Jia, Y.; Li, K.; Xue, L.; Ren, J.; Zhang, S.; Li, H. Mechanical and electromagnetic shielding performance of carbon fiber reinforced multilayered (PyC-SiC) n matrix composites. *Carbon* **2017**, *111*, 299–308. [[CrossRef](#)]
77. Voicu, V.; Pătru, I.; Dina, L.-A.; Nicolae, P.-M.; Smărăndescu, I.D. Shielding effectiveness evaluation using a non-standardized method. In Proceedings of the 2017 International Conference on Electromechanical and Power Systems (SIELMEN), Iasi, Romania, 11–13 October 2017.
78. Kashi, S.; Gupta, R.K.; Baum, T.; Kao, N.; Bhattacharya, S.N. Morphology, electromagnetic properties and electromagnetic interference shielding performance of poly lactide/graphene nanoplatelet nanocomposites. *Mater. Des.* **2016**, *95*, 119–126. [[CrossRef](#)]
79. Mittal, G.; Dhand, V.; Rhee, K.Y.; Park, S.-J.; Lee, W.R. A review on carbon nanotubes and graphene as fillers in reinforced polymer nanocomposites. *J. Ind. Eng. Chem.* **2015**, *21*, 11–25. [[CrossRef](#)]
80. Munalli, D.; Dimitrakis, G.; Chronopoulos, D.; Greedy, S.; Long, A. Electromagnetic shielding effectiveness of carbon fibre reinforced composites. *Compos. Part B Eng.* **2019**, *173*, 106906. [[CrossRef](#)]
81. Khalid, T.; Albasha, L.; Qaddoumi, N.; Yehia, S. Feasibility study of using electrically conductive concrete for electromagnetic shielding applications as a substitute for carbon-laced polyurethane absorbers in anechoic chambers. *IEEE Trans. Antennas Propag.* **2017**, *65*, 2428–2435. [[CrossRef](#)]
82. Kausar, A. Thermally conducting polymer/nanocarbon and polymer/inorganic nanoparticle nanocomposite: A review. *Polym. Plast. Technol. Mater.* **2020**, *59*, 895–909. [[CrossRef](#)]
83. Emerson, W. Electromagnetic wave absorbers and anechoic chambers through the years. *IEEE Trans. Antennas Propag.* **1973**, *21*, 484–490. [[CrossRef](#)]
84. He, K.; Yu, L.; Sheng, L.; An, K.; Ando, Y.; Zhao, X. Doping effect of single-wall carbon nanotubes on the microwave absorption properties of nanocrystalline barium ferrite. *Jpn. J. Appl. Phys.* **2010**, *49*, 125101. [[CrossRef](#)]
85. Zhang, H.-B.; Yan, Q.; Zheng, W.-G.; He, Z.; Yu, Z.-Z. Tough graphene–polymer microcellular foams for electromagnetic interference shielding. *ACS Appl. Mater. Interfaces* **2011**, *3*, 918–924. [[CrossRef](#)]

86. Zhang, N.; Wang, X.; Geng, L.; Liu, Z.; Zhang, X.; Li, C.; Zhang, D.; Wang, Z.; Zhao, G. Metallic Ni nanoparticles embedded in hierarchical mesoporous Ni(OH)<sub>2</sub>: A robust and magnetic recyclable catalyst for hydrogenation of 4-nitrophenol under mild conditions. *Polyhedron* **2019**, *164*, 7–12. [[CrossRef](#)]
87. Banerjee, R.; Gebrekstos, A.; Orasugh, J.T.; Ray, S.S. Nanocarbon-Containing Polymer Composite Foams: A Review of Systems for Applications in Electromagnetic Interference Shielding, Energy Storage, and Piezoresistive Sensors. *Ind. Eng. Chem. Res.* **2023**, *62*, 6807–6842. [[CrossRef](#)]
88. Wiroonpochit, P.; Keawmaungkom, S.; Chisti, Y.; Hansupalak, N. A novel preparation of natural rubber films with a conducting nanocarbon network for antistatic applications. *Mater. Today Commun.* **2023**, *34*, 105349. [[CrossRef](#)]
89. Kausar, A. Polymeric nanocomposite with polyhedral oligomeric silsesquioxane and nanocarbon (fullerene, graphene, carbon nanotube, nanodiamond)—Futuristic headways. *Polym.-Plast. Technol. Mater.* **2023**, *62*, 921–934. [[CrossRef](#)]
90. Rayar, A.; Naveen, C.; Onkarappa, H.; Betageri, V.S.; Prasanna, G. EMI shielding applications of PANI-Ferrite nanocomposite materials: A review. *Synth. Met.* **2023**, *295*, 117338. [[CrossRef](#)]
91. Idumah, C.I. Recent advancements in electromagnetic interference shielding of polymer and mxene nanocomposites. *Polym. Plast. Technol. Mater.* **2023**, *62*, 19–53. [[CrossRef](#)]
92. Kausar, A. Epitome of Fullerene in Conducting Polymeric Nanocomposite—Fundamentals and Beyond. *Polym. Plast. Technol. Mater.* **2023**, *62*, 618–631. [[CrossRef](#)]
93. Luo, J.; Wang, L.; Huang, X.; Li, B.; Guo, Z.; Song, X.; Lin, L.; Tang, L.-C.; Xue, H.; Gao, J. Mechanically durable, highly conductive, and anticorrosive composite fabrics with excellent self-cleaning performance for high-efficiency electromagnetic interference shielding. *ACS Appl. Mater. Interfaces* **2019**, *11*, 10883–10894. [[CrossRef](#)] [[PubMed](#)]
94. Zhou, X.; Jia, Z.; Feng, A.; Wang, X.; Liu, J.; Zhang, M.; Cao, H.; Wu, G. Synthesis of fish skin-derived 3D carbon foams with broadened bandwidth and excellent electromagnetic wave absorption performance. *Carbon* **2019**, *152*, 827–836. [[CrossRef](#)]
95. Sheldon, R.A. The E factor at 30: A passion for pollution prevention. *Green Chem.* **2023**, *25*, 1704–1728. [[CrossRef](#)]
96. Amin, A.; Wang, Z.; Shah, A.H.; Chandio, A.A. Exploring the dynamic nexus between renewable energy, poverty alleviation, and environmental pollution: Fresh evidence from E-9 countries. *Environ. Sci. Pollut. Res.* **2023**, *30*, 25773–25791. [[CrossRef](#)]
97. Zhu, C.; Wu, J.; Yan, J.; Liu, X. Advanced fiber materials for wearable electronics. *Adv. Fiber Mater.* **2023**, *5*, 12–35. [[CrossRef](#)]
98. Idumah, C.I. Recently emerging trends in flame retardancy of phosphorene polymeric nanocomposites and applications. *J. Anal. Appl. Pyrolysis* **2023**, *169*, 105855. [[CrossRef](#)]
99. Abubakre, O.K.; Medupin, R.O.; Akintunde, I.B.; Jimoh, O.T.; Abdulkareem, A.S.; Muriana, R.A.; James, J.A.; Ukoba, K.O.; Jen, T.-C.; Yoro, K.O. Carbon nanotube-reinforced polymer nanocomposites for sustainable biomedical applications: A review. *J. Sci. Adv. Mater. Devices* **2023**, *8*, 100557. [[CrossRef](#)]
100. Genix, A.-C.; Bocharova, V.; Carroll, B.; Dieudonné-George, P.; Chauveau, E.; Sokolov, A.P.; Oberdisse, J. How Tuning Interfaces Impacts the Dynamics and Structure of Polymer Nanocomposites Simultaneously. *ACS Appl. Mater. Interfaces* **2023**, *15*, 7496–7510. [[CrossRef](#)]
101. Huang, J.; Zhou, J.; Liu, M. Interphase in polymer nanocomposites. *JACS Au* **2022**, *2*, 280–291. [[CrossRef](#)]
102. Kamal, A.; Ashmawy, M.; Algazzar, A.M.; Elsheikh, A.H. Fabrication techniques of polymeric nanocomposites: A comprehensive review. *Proc. Inst. Mech. Eng. Part C J. Mech. Eng. Sci.* **2022**, *236*, 4843–4861. [[CrossRef](#)]
103. Gebrekstos, A.; Ray, S.S. Superior electrical conductivity and mechanical properties of phase-separated polymer blend composites by tuning the localization of nanoparticles for electromagnetic interference shielding applications. *J. Polym. Sci.* **2023**, *early view*. [[CrossRef](#)]
104. Siavashani, V.S.; Gursoy, N.C.; Montazer, M.; Altay, P. Stretchable electromagnetic interference shielding textile using conductive polymers and metal nanoparticles. *Fibers Polym.* **2022**, *23*, 2748–2759. [[CrossRef](#)]
105. Selvaraj, V.K.; Subramanian, J. A comparative study on bio-based PU foam reinforced with nanoparticles for EMI-shielding applications. *Polymers* **2022**, *14*, 3344. [[CrossRef](#)]
106. Wang, Y.-Y.; Zhang, F.; Li, N.; Shi, J.-F.; Jia, L.-C.; Yan, D.-X.; Li, Z.-M. Carbon-based aerogels and foams for electromagnetic interference shielding: A review. *Carbon* **2023**, *205*, 10–26. [[CrossRef](#)]
107. Deeraj, B.; Jayan, J.S.; Raman, A.; Saritha, A.; Joseph, K. Polymeric blends and nanocomposites for high performance EMI shielding and microwave absorbing applications. *Compos. Interfaces* **2022**, *29*, 1505–1547. [[CrossRef](#)]
108. Li, Y.-K.; Du, P.-Y.; Wang, Z.-X.; Huang, H.-D.; Jia, L.-C. Aramid nanofiber-induced assembly of graphene nanosheets toward highly thermostable and freestanding films for electromagnetic interference shielding. *Compos. Part A Appl. Sci. Manuf.* **2022**, *160*, 107063. [[CrossRef](#)]
109. Das, M.; Sethy, P.P.; Sundaray, B. EMI shielding performance of graphene oxide reinforced polyaniline/polystyrene solution cast thin films. *Synth. Met.* **2023**, *296*, 117369. [[CrossRef](#)]
110. Yue, L.; Jayapal, M.; Cheng, X.; Zhang, T.; Chen, J.; Ma, X.; Dai, X.; Lu, H.; Guan, R.; Zhang, W. Highly dispersed ultra-small nano Sn-SnSb nanoparticles anchored on N-doped graphene sheets as high performance anode for sodium ion batteries. *Appl. Surf. Sci.* **2020**, *512*, 145686. [[CrossRef](#)]
111. Zheng, X.; Zhang, H.; Liu, Z.; Jiang, R.; Zhou, X. Functional composite electromagnetic shielding materials for aerospace, electronics and wearable fields. *Mater. Today Commun.* **2022**, *33*, 104498. [[CrossRef](#)]
112. Al-Amri, A.M. Recent Progress in Printed Photonic Devices: A Brief Review of Materials, Devices, and Applications. *Polymers* **2023**, *15*, 3234. [[CrossRef](#)]

113. Chen, Y.; Li, Y.; Yip, M.; Tai, N. Electromagnetic interference shielding efficiency of polyaniline composites filled with graphene decorated with metallic nanoparticles. *Compos. Sci. Technol.* **2013**, *80*, 80–86. [[CrossRef](#)]
114. Modak, P.; Kondawar, S.B.; Nandanwar, D. Synthesis and characterization of conducting polyaniline/graphene nanocomposites for electromagnetic interference shielding. *Procedia Mater. Sci.* **2015**, *10*, 588–594. [[CrossRef](#)]
115. Shen, B.; Li, Y.; Yi, D.; Zhai, W.; Wei, X.; Zheng, W. Strong flexible polymer/graphene composite films with 3D saw-tooth folding for enhanced and tunable electromagnetic shielding. *Carbon* **2017**, *113*, 55–62. [[CrossRef](#)]
116. Khasim, S. Polyaniline-Graphene nanoplatelet composite films with improved conductivity for high performance X-band microwave shielding applications. *Results Phys.* **2019**, *12*, 1073–1081. [[CrossRef](#)]
117. Xue, L.; Zhang, H.; Zhou, Z.; Bi, K. Fabrication and Electromagnetic Interference Shielding Properties of a Fe<sub>3</sub>O<sub>4</sub>/Polythiophene/Au Nanocomposite Film Coated by Epoxy Resin. In Proceedings of the 2023 IEEE 18th International Conference on Nano/Micro Engineered and Molecular Systems (NEMS), Jeju Island, Republic of Korea, 14–17 May 2023.
118. Joshi, A.; Srivastava, R.; Dhyani, R.; Joshi, C.S. Structural, magnetic, and dielectric properties of yttrium doped cobalt ferrite and their nanocomposites with polythiophene. *J. Magn. Magn. Mater.* **2023**, *578*, 170812. [[CrossRef](#)]
119. Chen, C.; Feng, W.; Wu, W.; Yu, Y.; Qian, G.; Fu, L.; Min, D. A highly strong PEDOT modified wood towards efficient electromagnetic interference shielding. *Ind. Crops Prod.* **2023**, *202*, 117109. [[CrossRef](#)]
120. Orasugh, J.T.; Ray, S.S. Functional and Structural Facts of Effective Electromagnetic Interference Shielding Materials: A Review. *ACS Omega* **2023**, *8*, 8134–8158. [[CrossRef](#)]
121. Guo, R.; Li, B.; Lu, T.; Lin, T.; Andre, J.; Zhang, C.; Zhi, L.; Chen, Z. Molecular Orientations at Buried Conducting Polymer/Graphene Interfaces. *Macromolecules* **2021**, *54*, 4050–4060. [[CrossRef](#)]
122. Jalali, A.; Zhang, R.; Rahmati, R.; Nofar, M.; Sain, M.; Park, C.B. Recent progress and perspective in additive manufacturing of EMI shielding functional polymer nanocomposites. *Nano Res.* **2023**, *16*, 1–17. [[CrossRef](#)]
123. Revanasiddappa, M.; Nayak, H.; Marudhachalam, N.; Venkatasubramanian, A.K.C.; Chandra, A.R.A.; Iyyappan, A.M.; Krishna, S.B.N. Nanoclay-Based Conductive and EMI Shielding Properties of Silver-Decorated Polyaniline and Its Nanocomposites. *Mater. Adv.* **2023**, 1–9. [[CrossRef](#)]
124. Nimra, S.S.; Rehan, Z.; Ali, S.H.; Atir, S.; Fatima, K.; Shahzadi, F.; Shakir, H.F.; Alamir, M.A.; EL-Bagory, T.M.A.A.; Shahid, I. Electrically conductive fibers fabrication and characterization via in-situ polymerization of aniline for the protection against EMI and thermal imaging signals. *J. Mater. Res. Technol.* **2023**, *23*, 2399–2409. [[CrossRef](#)]
125. Wang, Z.; Zhang, X.; Cheng, C.; Song, X.; Hua, C.; Feng, L.; Yang, J.; Jiang, J.; Liu, Y. 3D Printed Epoxy Composite Microsandwich with High Strength, Toughness, and EMI Shielding Performances. *Compos. Struct.* **2023**, *323*, 117456. [[CrossRef](#)]
126. Yun, J.; Zhou, C.; Guo, B.; Wang, F.; Zhou, Y.; Ma, Z.; Qin, J. Mechanically strong and multifunctional nano-nickel aerogels based epoxy composites for ultra-high electromagnetic interference shielding and thermal management. *J. Mater. Res. Technol.* **2023**, *24*, 9644–9656. [[CrossRef](#)]
127. Duan, N.; Shi, Z.; Wang, J.; Zhang, X.; Zhang, C.; Zhang, C.; Wang, G. Multilayer-structured carbon fiber fabric/graphene oxide/Fe<sub>3</sub>O<sub>4</sub>/epoxy composite for highly efficient mechanical and electromagnetic interference shielding. *Appl. Surf. Sci.* **2023**, *613*, 156038. [[CrossRef](#)]
128. Bheema, R.K.; Etika, K.C. The influence of hybrid decorated structures on the EMI shielding properties of epoxy composites over the X-Band. *Mater. Today Proc.* **2023**, *76*, 398–402. [[CrossRef](#)]
129. Wei, L.; Zhang, W.; Ma, J.; Bai, S.-L.; Ren, Y.; Liu, C.; Simion, D.; Qin, J.  $\pi$ - $\pi$  stacking interface design for improving the strength and electromagnetic interference shielding of ultrathin and flexible water-borne polymer/sulfonated graphene composites. *Carbon* **2019**, *149*, 679–692. [[CrossRef](#)]
130. Hamidinejad, M.; Zhao, B.; Zandieh, A.; Moghimian, N.; Filleter, T.; Park, C.B. Enhanced electrical and electromagnetic interference shielding properties of polymer-graphene nanoplatelet composites fabricated via supercritical-fluid treatment and physical foaming. *ACS Appl. Mater. Interfaces* **2018**, *10*, 30752–30761. [[CrossRef](#)]
131. Anderson, L.; Govindaraj, P.; Ang, A.; Mirabedini, A.; Hameed, N. Modelling, Fabrication and Characterization of Graphene/Polymer Nanocomposites for Electromagnetic Interference Shielding Applications. *Carbon Trends* **2021**, *4*, 100047. [[CrossRef](#)]
132. Pavlou, C.; Pastore Carbone, M.G.; Manikas, A.C.; Trakakis, G.; Koral, C.; Papari, G.; Andreone, A.; Galiotis, C. Effective EMI shielding behaviour of thin graphene/PMMA nanolaminates in the THz range. *Nat. Commun.* **2021**, *12*, 4655. [[CrossRef](#)]
133. Lakshmi, N.; Tambe, P. EMI shielding effectiveness of graphene decorated with graphene quantum dots and silver nanoparticles reinforced PVDF nanocomposites. *Compos. Interfaces* **2017**, *24*, 861–882. [[CrossRef](#)]
134. Zhang, H.; Zhang, G.; Gao, Q.; Zong, M.; Wang, M.; Qin, J. Electrically electromagnetic interference shielding microcellular composite foams with 3D hierarchical graphene-carbon nanotube hybrids. *Compos. Part A Appl. Sci. Manuf.* **2020**, *130*, 105773. [[CrossRef](#)]
135. Zhu, S.; Cheng, Q.; Yu, C.; Pan, X.; Zuo, X.; Liu, J.; Chen, M.; Li, W.; Li, Q.; Liu, L. Flexible Fe<sub>3</sub>O<sub>4</sub>/graphene foam/polydimethylsiloxane composite for high-performance electromagnetic interference shielding. *Compos. Sci. Technol.* **2020**, *189*, 108012. [[CrossRef](#)]
136. Jia, H.; Kong, Q.-Q.; Liu, Z.; Wei, X.-X.; Li, X.-M.; Chen, J.-P.; Li, F.; Yang, X.; Sun, G.-H.; Chen, C.-M. 3D graphene/carbon nanotubes/polydimethylsiloxane composites as high-performance electromagnetic shielding material in X-band. *Compos. Part A Appl. Sci. Manuf.* **2020**, *129*, 105712. [[CrossRef](#)]

137. Liang, C.; Hamidinejad, M.; Ma, L.; Wang, Z.; Park, C.B. Lightweight and flexible graphene/SiC-nanowires/poly (vinylidene fluoride) composites for electromagnetic interference shielding and thermal management. *Carbon* **2020**, *156*, 58–66. [[CrossRef](#)]
138. Cheng, K.; Li, H.; Zhu, M.; Qiu, H.; Yang, J. In situ polymerization of graphene-polyaniline@ polyimide composite films with high EMI shielding and electrical properties. *RSC Adv.* **2020**, *10*, 2368–2377. [[CrossRef](#)]
139. Liu, Q.; He, X.; Yi, C.; Sun, D.; Chen, J.; Wang, D.; Liu, K.; Li, M. Fabrication of ultra-light nickel/graphene composite foam with 3D interpenetrating network for high-performance electromagnetic interference shielding. *Compos. Part B Eng.* **2020**, *182*, 107614. [[CrossRef](#)]
140. Song, P.; Qiu, H.; Wang, L.; Liu, X.; Zhang, Y.; Zhang, J.; Kong, J.; Gu, J. Honeycomb structural rGO-MXene/epoxy nanocomposites for superior electromagnetic interference shielding performance. *Sustain. Mater. Technol.* **2020**, *24*, e00153. [[CrossRef](#)]
141. Navik, R.; Tan, H.; Zhang, H.; Liu, Z.; Xiang, Q.; Shi, L.; Lu, S.; Zhao, Y. Scalable production of polyamide-6/graphene composites with enhanced electromagnetic shielding and thermal conductivity. *Chem. Eng. J.* **2023**, *471*, 144445. [[CrossRef](#)]
142. Cao, M.S.; Shu, J.C.; Wang, X.X.; Wang, X.; Zhang, M.; Yang, H.J.; Fang, X.Y.; Yuan, J. Electronic structure and electromagnetic properties for 2D electromagnetic functional materials in gigahertz frequency. *Ann. Phys.* **2019**, *531*, 1800390. [[CrossRef](#)]
143. Ge, X.; Chai, Z.; Shi, Q.; Liu, Y.; Wang, W. Graphene superlubricity: A review. *Friction* **2023**, *11*, 1953–1973. [[CrossRef](#)]
144. Jia, L.C.; Yan, D.X.; Yang, Y.; Zhou, D.; Cui, C.H.; Bianco, E.; Lou, J.; Vajtai, R.; Li, B.; Ajayan, P.M. High strain tolerant EMI shielding using carbon nanotube network stabilized rubber composite. *Adv. Mater. Technol.* **2017**, *2*, 1700078. [[CrossRef](#)]
145. Wang, R.; Sun, L.; Zhu, X.; Ge, W.; Li, H.; Li, Z.; Zhang, H.; Huang, Y.; Li, Z.; Zhang, Y.F. Carbon nanotube-based strain sensors: Structures, fabrication, and applications. *Adv. Mater. Technol.* **2023**, *8*, 2200855. [[CrossRef](#)]
146. Huang, C.L.; Yang, H.P.; Ye, J.Y.; Fan, Y.C.; Huang, S.P. The cocontinuous morphology induced from the graphene nanosheets percolation network structures in the immiscible high density polyethylene/polyamide 6/graphene nanosheets composites. *Polym. Compos.* **2023**, *44*, 4955–4975. [[CrossRef](#)]
147. Haghgoo, M.; Ansari, R.; Jang, S.-H.; Hassanzadeh-Aghdam, M.K.; Nankali, M. Developing a high-efficiency predictive model for self-temperature-compensated piezoresistive properties of carbon nanotube/graphene nanoplatelet polymer-based nanocomposites. *Compos. Part A Appl. Sci. Manuf.* **2023**, *166*, 107380. [[CrossRef](#)]
148. Zare, Y.; Gharib, N.; Nam, D.-H.; Chang, Y.-W. Predicting of tunneling resistivity between adjacent nanosheets in graphene-polymer systems. *Sci. Rep.* **2023**, *13*, 12455. [[CrossRef](#)]
149. Xie, Z.; Chen, H.; Hu, S.; Zhao, H.; Chen, W.; Jiang, D. Graphene/carbon nanotube/polypyrrole composite films for electromagnetic interference shielding. *Polym. Compos.* **2023**, *44*, 3798–3807. [[CrossRef](#)]
150. Tarhini, A.; Tehrani-Bagha, A. Advances in Preparation Methods and Conductivity Properties of Graphene-based Polymer Composites. *Appl. Compos. Mater.* **2023**, 1–26. [[CrossRef](#)]
151. Rath, R.; Mohanty, S.; Kumar, P.; Nayak, S.K.; Unnikrishnan, L. Synergistic effect of silica-covered graphene oxide (in-situ) hybrid nanocomposites for use as a polymer electrolyte membrane for fuel cell applications. *Surf. Interfaces* **2023**, *38*, 102761. [[CrossRef](#)]
152. Novikov, A.S. Non-Covalent Interactions in Polymers. *Polymers* **2023**, *15*, 1139. [[CrossRef](#)]
153. Fu, X.; Lin, J.; Liang, Z.; Yao, R.; Wu, W.; Fang, Z.; Zou, W.; Wu, Z.; Ning, H.; Peng, J. Graphene oxide as a promising nanofiller for polymer composite. *Surf. Interfaces* **2023**, *37*, 102747. [[CrossRef](#)]
154. Ma, J.; Meng, Q.; Michelmores, A.; Kawashima, N.; Izzuddin, Z.; Bengtsson, C.; Kuan, H.-C. Covalently bonded interfaces for polymer/graphene composites. *J. Mater. Chem. A* **2013**, *1*, 4255–4264. [[CrossRef](#)]
155. Shen, B.; Zhai, W.; Tao, M.; Lu, D.; Zheng, W. Chemical functionalization of graphene oxide toward the tailoring of the interface in polymer composites. *Compos. Sci. Technol.* **2013**, *77*, 87–94. [[CrossRef](#)]
156. Omana, L.; Chandran, A.; John, R.E.; Wilson, R.; George, K.C.; Unnikrishnan, N.V.; Varghese, S.S.; George, G.; Simon, S.M.; Paul, I. Recent advances in polymer nanocomposites for electromagnetic interference shielding: A Review. *ACS Omega* **2022**, *7*, 25921–25947. [[CrossRef](#)]
157. Tian, K.; Hu, D.; Wei, Q.; Fu, Q.; Deng, H. Recent progress on multifunctional electromagnetic interference shielding polymer composites. *J. Mater. Sci. Technol.* **2023**, *134*, 106–131. [[CrossRef](#)]
158. Shahzad, F.; Alhabeab, M.; Hatter, C.B.; Anasori, B.; Hong, S.M.; Koo, C.M.; Gogotsi, Y. Electromagnetic interference shielding with 2D transition metal carbides (MXenes). *Science* **2016**, *353*, 1137–1140. [[CrossRef](#)] [[PubMed](#)]
159. Ghosh, S.; Ganguly, S.; Das, P.; Das, T.K.; Bose, M.; Singha, N.K.; Das, A.K.; Das, N.C. Fabrication of reduced graphene oxide/silver nanoparticles decorated conductive cotton fabric for high performing electromagnetic interference shielding and antibacterial application. *Fibers Polym.* **2019**, *20*, 1161–1171. [[CrossRef](#)]
160. Lin, C.-L.; Li, J.-W.; Chen, Y.-F.; Chen, J.-X.; Cheng, C.-C.; Chiu, C.-W. Graphene Nanoplatelet/Multiwalled Carbon Nanotube/Polypyrrole Hybrid Fillers in Polyurethane Nanohybrids with 3D Conductive Networks for EMI Shielding. *ACS Omega* **2022**, *7*, 45697–45707. [[CrossRef](#)]
161. Mondal, S.; Ganguly, S.; Das, P.; Khastgir, D.; Das, N.C. Low percolation threshold and electromagnetic shielding effectiveness of nano-structured carbon based ethylene methyl acrylate nanocomposites. *Compos. Part B Eng.* **2017**, *119*, 41–56. [[CrossRef](#)]
162. You, X.; Zhang, Q.; Yang, J.; Dong, S. Review on 3D-printed graphene-reinforced composites for structural applications. *Compos. Part A Appl. Sci. Manuf.* **2023**, *167*, 107420. [[CrossRef](#)]
163. Moussa, M.; El-Kady, M.F.; Zhao, Z.; Majewski, P.; Ma, J. Recent progress and performance evaluation for polyaniline/graphene nanocomposites as supercapacitor electrodes. *Nanotechnology* **2016**, *27*, 442001. [[CrossRef](#)]

164. Weerasinghe, A.; Lu, C.-T.; Maroudas, D.; Ramasubramaniam, A. Multiscale shear-lag analysis of stiffness enhancement in polymer–graphene nanocomposites. *ACS Appl. Mater. Interfaces* **2017**, *9*, 23092–23098. [[CrossRef](#)]
165. Sun, J.; Zhou, D. Advances in Graphene–Polymer Nanocomposite Foams for Electromagnetic Interference Shielding. *Polymers* **2023**, *15*, 3235. [[CrossRef](#)]
166. Cheng, Z.; Wang, R.; Wang, Y.; Cao, Y.; Shen, Y.; Huang, Y.; Chen, Y. Recent advances in graphene aerogels as absorption-dominated electromagnetic interference shielding materials. *Carbon* **2023**, *205*, 112–137. [[CrossRef](#)]
167. Li, Y.-K.; Li, W.-J.; Wang, Z.-X.; Du, P.-Y.; Xu, L.; Jia, L.-C.; Yan, D.-X. High-efficiency electromagnetic interference shielding and thermal management of high-graphene nanoplate-loaded composites enabled by polymer-infiltrated technique. *Carbon* **2023**, *211*, 118096. [[CrossRef](#)]
168. Abbasi, H.; Antunes, M.; Velasco, J.I. Recent advances in carbon-based polymer nanocomposites for electromagnetic interference shielding. *Prog. Mater. Sci.* **2019**, *103*, 319–373. [[CrossRef](#)]
169. Wu, G.; Jia, Z.; Zhou, X.; Nie, G.; Lv, H. Interlayer controllable of hierarchical MWCNTs@C@FexOy cross-linked composite with wideband electromagnetic absorption performance. *Compos. Part A Appl. Sci. Manuf.* **2020**, *128*, 105687. [[CrossRef](#)]
170. Manthiram, A. An outlook on lithium ion battery technology. *ACS Cent. Sci.* **2017**, *3*, 1063–1069. [[CrossRef](#)] [[PubMed](#)]
171. Yu, L.; Lan, X.; Wei, C.; Li, X.; Qi, X.; Xu, T.; Li, C.; Li, C.; Wang, Z. MWCNT/NiO-Fe<sub>3</sub>O<sub>4</sub> hybrid nanotubes for efficient electromagnetic wave absorption. *J. Alloys Compd.* **2018**, *748*, 111–116. [[CrossRef](#)]

**Disclaimer/Publisher’s Note:** The statements, opinions and data contained in all publications are solely those of the individual author(s) and contributor(s) and not of MDPI and/or the editor(s). MDPI and/or the editor(s) disclaim responsibility for any injury to people or property resulting from any ideas, methods, instructions or products referred to in the content.